Article

Hydrogeochemical Characteristics and Formation Processes of Ordovician Limestone Groundwater in Zhuozishan Coalfield, Northwest China

Shidong Wang [1,2], **Tiantian Wang** [1,2,*] iD, **Zhibin Yang** [1,2], **Hongwei Tang** [1,2], **Hanjiang Lv** [1,2], **Feng Xu** [1,2], **Kaipeng Zhu** [1,2] and **Ziyuan Liu** [1,2]

1 Technology & Engineering, Xi'an Research Institute of China Coal (Group), Corp, Xi'an 710077, China
2 Key Laboratory of Coal Mine Water Hazard Prevention and Control Technology in Shaanxi Province, Xi'an 710054, China
* Correspondence: wangthpuedu@126.com

Abstract: A comprehensive understanding of the characteristics and formation mechanisms of groundwater in mining areas is essential for the effective prevention of coal mine water and the rational management of groundwater resources. The objective of this study was to examine the hydrogeochemical characteristics and evolution of Ordovician groundwater in the Zhuozishan coal mine, located in the northwest region of China. A total of 34 groundwater samples were collected for hydrogeochemical analyses and the investigation of their evolution processes, with the aid of a piper trilinear diagram, a Gibbs diagram, and an ion ratio diagram. The results indicate that the concentration of sodium (Na^+), potassium (K^+), bicarbonate (HCO_3^-), chloride (Cl^-), sulphate (SO_4^{2-}), total dissolved solids (TDS), and pH increases from the recharge area to the discharge area, whereas the concentration of calcium (Ca^{2+}) and magnesium (Mg^{2+}) decreases. The hydrogeochemical characteristics of the runoff from Zhuozishan to Gongdeer coalfield and further southward display a notable north–south directional change. The groundwater process is primarily controlled by rock weathering action and cation exchange, with Na^+ and K^+ deriving primarily from cation exchange and only to a minor extent from halite dissolution. In conclusion, the northern part of the coalfield is characterised by a geological structure that creates a retention area with groundwater, resulting in an unordered runoff process with a complex formation mechanism. The middle region is devoid of geological constraints that would alter the flow direction, thus simplifying the process of groundwater formation. In contrast, the southern area experiences an increase in strata depth and fault blocking, which creates a retention zone, thereby rendering the groundwater formation process more complex. This research contributes to the effective management of groundwater resources in this coalfield and other mining sites.

Keywords: coal mining; groundwater hydrogeochemical characteristics; hydrogeochemical; Zhuoizishan coalfield

1. Introduction

In recent years, the global demand for fresh groundwater has escalated significantly due to rapid population growth, industrial expansion, and the intensification of agricultural irrigation activities [1,2]. This heightened demand has put immense pressure on groundwater resources, particularly in regions where these resources are already scarce or vulnerable to depletion [3–5]. These issues arise from a combination of natural processes and anthropogenic activities, particularly those related to extensive groundwater extraction and mining operations.

In the context of coal mining, large volumes of groundwater are often discharged from mine shafts and pits, leading to a significant decline in local groundwater levels [6–8]. This discharge can also induce hydraulic connectivity between different aquifers, thereby

facilitating the migration of contaminants and resulting in widespread water quality deterioration [9]. The impact of mining activities on groundwater is thus profound, affecting both the quantity and quality of this vital resource. Understanding the geochemical characteristics and processes governing groundwater in mining regions is therefore crucial for assessing the long-term sustainability of groundwater resources and for developing effective management strategies [10].

China, with its vast coal reserves, stands as the world's leading producer and consumer of coal [5,9]. In 2019, China's coal consumption reached a staggering 2.22 billion tons, accounting for 57.7% of the country's total energy consumption [10]. However, the hydrogeological conditions underlying many of China's coal mines are complex and challenging, making these areas particularly susceptible to groundwater-related hazards, including mine water inrush incidents. From 2000 to 2014, China reported over 4500 fatalities linked to mine water inrush events, underscoring the severity of the issue [5,9]. For an extended period, techniques such as hydrochemical analysis, water quality type comparison, and multivariate statistical analysis can be effectively employed to ascertain the nature of the water inrush source at the outset of the water inrush [11,12]. This method is very effective in avoiding mine water inrush disasters.

On the one hand, the Zhuozishan coalfield, located in the westernmost region of the Ordos Basin, is one such area where the hydrogeological challenges are pronounced. The coal seams in this region are primarily located within carboniferous and Permian formations, with the Ordovician limestone aquifer posing the greatest hazard due to its potential to contribute to mine water gushing-out events. A notable incident occurred in 2010 at the Luotuoshan mine within the Zhuozishan coalfield, where a catastrophic water inrush event led to a peak inflow of 60,036 m^3/h metres per hour, causing extensive economic losses and endangering human lives. This event highlighted the critical need for a thorough understanding of the hydrochemical characteristics of groundwater in the region, as such knowledge is essential for identifying potential mine water sources and implementing preventive measures against water inrushes.

On the other hand, the Zhuozishan coalfield, which falls under the jurisdiction of the Wuhai administrative region, is situated in an arid to semi-arid climatic zone. These climatic conditions contribute to the scarcity of surface water, making groundwater the most crucial resource for meeting the drinking, domestic, and industrial water demands of Wuhai city. Notably, groundwater accounts for 42.4% of the municipal water supply, with 8% specifically sourced from the drainage of Ordovician limestone in the Zhuozishan coalfield [12]. As coal mining activities in the Zhuozishan coalfield continue to intensify, the volume of groundwater drainage from the Ordovician limestone is expected to increase correspondingly. This trend underscores the growing importance of this groundwater source for the future economic development of Wuhai city. Therefore, research on the hydrochemical characteristics and formation mechanism of the Ordovician limestone aquifer in the Zhuozishan coalfield can help scientific planning and the effective use and protection of groundwater resources in the coalfield area.

2. Material and Method

2.1. Study Area

The Zhuozishan coal mine represents a significant coal mining district within the Ordos Basin. The mine is situated between the Zhuozishan and Gangdeer coalfield, spanning a longitudinal range of 107°2′15″–107°5′45″ and a latitudinal range of 39°21′15″–39°22′41″. The Zhuozishan coalfield is currently composed of ten distinct mining areas, each bearing the name of a local village: Kabuqi, Pinggou, Luotuoshan, Baiyinwusu, Dilibangwusu, Tianyu, Hairong, Zhengfeng, Limin, and Qipanjing.

The region is characterised by aridity and semi-aridity, with significant temperature fluctuations. The annual average temperature is 7.6 °C, with a daily maximum and minimum air temperature of 36.7 °C and −31.6 °C, respectively [13]. The annual precipitation is 140 mm, while the annual evaporation is 3600 mm per year [14]. Evaporation is therefore approximately 25 times greater than precipitation. Furthermore, the area has limited surface water resources, which highlights the importance of groundwater in this region.

2.2. Hydrogeological Condition

The Zhuozishan coalfield is located in Wuhai City, Inner Mongolia Autonomous Region, and the mining area is mainly distributed between Zhuozishan and Gangdel Mountain and the southern part of Zhuozishan, with the main mining of Carboniferous and Permian coal seams (Figure 1b). The Zhuozishan coalfield is an independent karst groundwater system belonging to the Cambrian–Ordovician carbonate karst groundwater system in the Ordos Basin, and it is divided into four independent water circulation systems according to the characteristics of local hydraulic connection, water volume distribution, and replenishment conditions: the Qianli Mountain karst water subsystem (I), the Gondel Mountain karst water subsystem (II), the Zhuozishan north section karst water subsystem (III), the Zhuozishan south section karst water subsystem (II), and the southern section of the Zhuozishan karst water subsystem (IV) (Figure 1a).
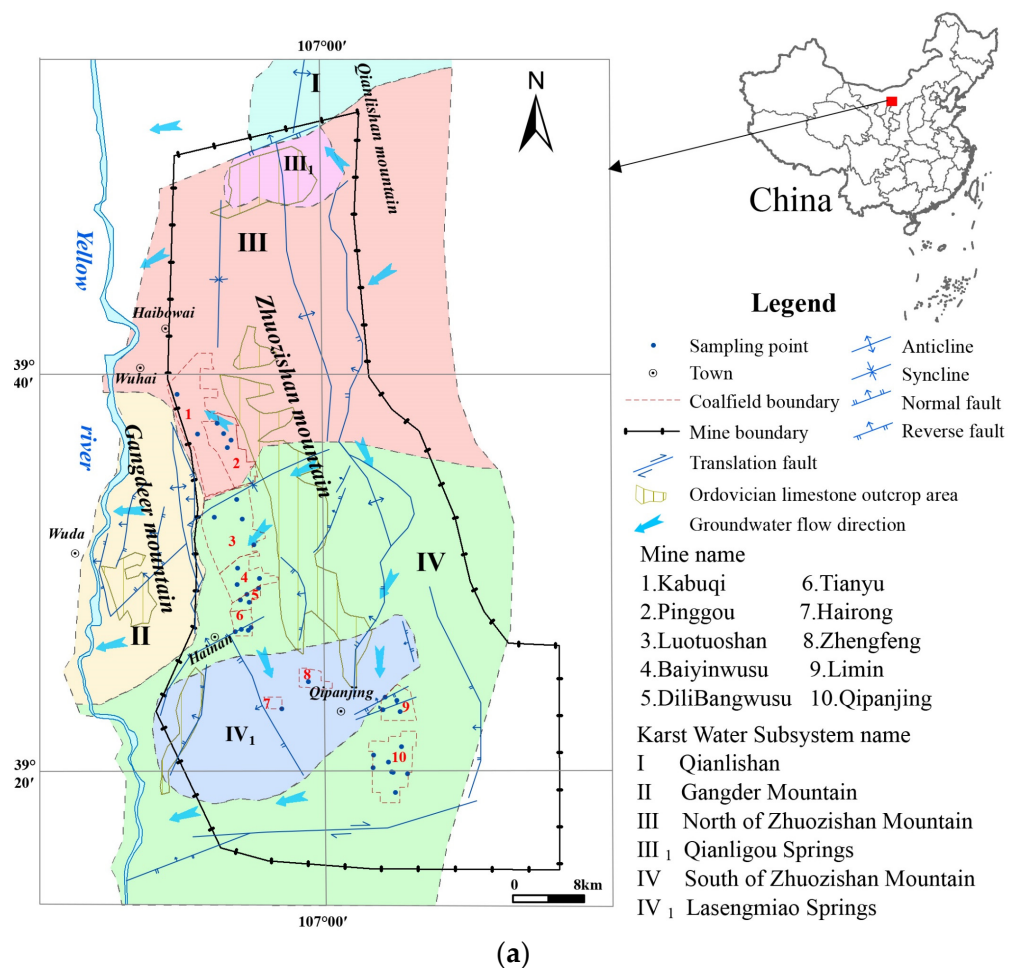

(a)

Figure 1. *Cont.*

Sytem	Symbol	Column	Thickness(m)	Lithology
Quaternary	Q		0-29.73	Dominated by a gravel layer and sandy soils
Paleogene	E		31.10-235.11	Sandy conglomerate with interbedded sandy mudstone clasts
Permian	P_2s		109.26-156.96	Coarse sandstone in the upper part, sandy mudstone in the middle, medium and coarse sandstone in the lower part
	P_1x		17.42-44.44	Coarse and medium fine sandstone interbedded with coloured sandy mud;
	P_1s	No.3 No.5 No.9 No.16	33.35-78.59	Sandy mudstone and coarse and medium sandstone in the upper part, medium and fine sandstone in the middle, and fine sandstone and sandy mudstone in the lower part, interbedded with coal seams
Carboniferous	C_2t		12 92-64.88	Dark grey sandy mudstone and mudstone in the upper part and greyish-white, light grey medium and fine grained sandstone in the lower part, interbedded with coal seams
Ordovician	O_1s		Thicker	Sandy mudstone, mudstone, sandstone, mudstone, sandstone, greyish-white calcareous quartz sandstone

(**b**)

Figure 1. Overview of Ordovician limestone groundwater in Zhuozishan coalfield (**a**) and composite stratigraphic column of the study area (**b**).

The coalfield is located in the northwestern part of China, where surface rivers are sparse and have low flow rates. As a result, atmospheric precipitation becomes the primary source of recharge for the Ordovician aquifer. The water level elevation of the Ordovician limestone aquifer is 1009.40–1024.47 m. Precipitation primarily recharges the aquifer in the exposed limestone area of the Zhuozishan region, from where it flows westward, crossing the Kabuchi syncline before reaching the eastern edge of the Gangdeleshan mountain range (Figure 2b1,b2). The flow is obstructed by water-blocking faults, causing the flow direction to change to north–south within the syncline. Eventually, the groundwater either discharges as springs or flows laterally towards the Yellow River, effectively dividing the Zhuozishan into two karst water subsystems, north and south, by the Kabuchi syncline.

On the other hand, groundwater also flows southward from Zhuozishan. However, due to the increasing depth of strata in the south and the obstruction caused by the Zhengyiguan strike-slip fault, a retention zone is formed, leading the groundwater to eventually discharge as springs or flow laterally towards the Yellow River (Figure 2a). Due to the limited recharge of Ordovician limestone groundwater, the groundwater circulation is relatively slow. Only in areas with karst fault structures and deeply incised karst valleys do strong runoff zones form.

2.3. Water Sampling and Analysis

A total of 34 Ordovician limestone groundwater samples were randomly collected from the 10 mining areas within the Zhuozishan coalfield. The precise locations from which samples were taken are illustrated in Figure 1. The sampling and preservation methods and processes adhered to the national standard [15]. Prior to the collection of water samples, the bottles were rinsed three times. At each sampling location, two 1 L plastic bottles were filled. One sample was utilised for cation and anion analyses, while the other was employed for in situ testing. The TDS and pH values were immediately measured in the field using a portable conductivity and pH meter (Shanghai Sanxin Company, Shanghai, China). Subsequently, the sampling bottles were labelled, sealed, and transported to the laboratory of coal mine water hazard prevention and control technology in Shaanxi Province for cation and anion determinations within 24 h. In the laboratory, all water samples were filtered through 0.45 μm millipore membrane filters prior to testing. The concentrations of anions (chloride, sulphate) were determined by anion chromatography

with anion columns (Thermo Company, Waltham, MA, USA), while cations (calcium, magnesium, sodium, potassium) were measured by cation chromatography with cation columns. Furthermore, the analysis of HCO3 was conducted using the titrimetric method. The accuracy of the analysis was verified through the use of a water reference standard (NIST 1643b). In the majority of cases, the precision obtained was better than 5% RSD, with comparable accuracy.
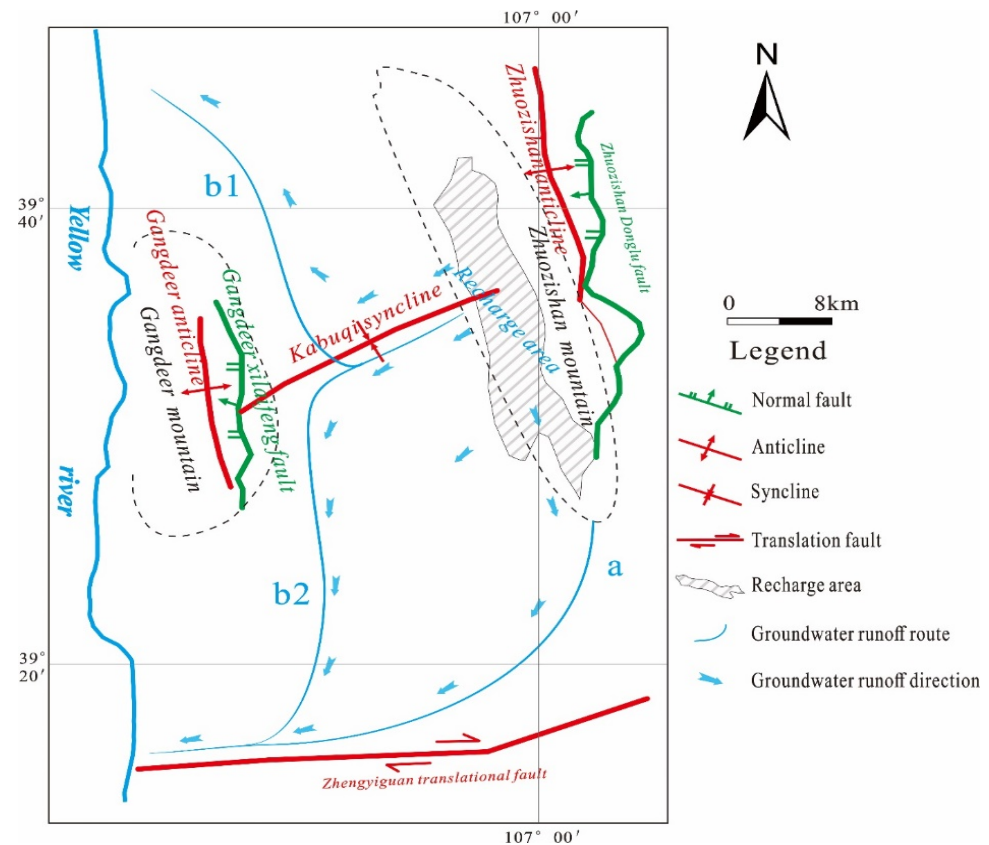

Figure 2. Recharge runoff and discharge conditions of Ordovician limestone groundwater.

3. Results

3.1. General Hydrochemistry

The principal cations and anions present in the sampled water sources are presented in Table 1. As illustrated in the table, the pH of all groundwater samples exhibited a range from 7.01 (neutral) to 7.78 (slightly alkaline). The total dissolved solids (TDSs) of the groundwater samples exhibited a range of 464.75 to 3366.52 milligrammes per litre (mg/L). The predominant cations in the limestone groundwater were sodium (Na^+) and calcium (Ca^{2+}). The concentration of sodium ions (Na^+) was found to vary from 35.19 to 900.40 mg/L. The concentration of calcium ranged from 27.61 to 603.51 mg/L (with an average of 61.21 mg/L), while that of magnesium varied from 4.5 to 133.46 mg/L.

Table 1. The results of water sample testing.

Number	Mine	K$^+$	Na$^+$	Ca^{2+}	Mg^{2+}	HCO$_3^-$	SO$_4^{2-}$	Cl$^-$	pH	EC (μS/cm)
1	Kabuqi	7.77	176.57	37.5	26.53	277.78	169.58	137.76	7.75	1303.13
2		10.87	160	102.35	39.8	402.05	27.58	255.1	8.4	1604.79
3	Pinggou	1.5	230	59.17	18.63	188.45	330.93	123.78	7.85	1555.77
4		5.95	147	157.78	61.61	255.72	209.92	353.66	7.35	1914.817
5		4.28	250	90.72	54.45	258.62	249.43	353.66	7.57	2005.55
6		7.68	149	123.44	69.17	274.13	389.37	195.94	8.18	1945.20
7	Luotuoshan	32	489	52.86	63.04	247.02	555.66	503.97	8.1	3062.5
8		3	61.25	67.06	35.34	218.03	117.55	88.42	7.4	937.5
9		6.4	35.19	95.4	51.97	126.09	118.13	88.42	8.45	798.44
10		3.55	68	59.38	34.59	240	109.07	86.84	8.25	971
11	Baiyinwusu	2.2	197	603.51	23.4	32.47	213.21	1237.81	8.8	3649.08
12		6.2	288	35.5	23.4	211.65	190.98	282.93	7.77	1644.06
13		3.4	58.9	27.61	47.28	55.67	126.77	114.94	8.35	726.17
14	Dilibangwusu	2.04	76.65	65.99	32.29	265.03	108.86	82.99	8.15	1005.48
15		2.56	63.5	67.86	22.31	270.3	80.65	62.17	7.01	907.81
16		3.08	63.47	58.14	30.07	275.72	90.97	68.83	7.66	933.36
17	Tianyu	2.94	74.2	73.59	26.28	264	102.6	79.5	7.48	989.06
18		1.49	63.52	54.88	28.12	232.24	88.1	72.21	8.22	871.11
19		4.32	80	59.6	26.08	267.2	97.75	76.02	7.76	971.88
20		0.66	101.43	99.43	44.23	296.56	136.86	99.37	7.3	1325.77
21	Hairong	2.32	210.05	77.51	40.24	271.29	217.34	205.8	7.77	1664.06
22	Zhengfeng	3.84	112.2	67.5	34.71	287	200.9	62.5	7.76	1221.88
23	Limin	29.8	230	63.11	42.51	249.92	293.88	247.56	7.95	1849.98
24		2	254	27.61	25.79	110.17	229.67	176.83	8.09	1440.91
25		3.2	425	59.17	40.12	226.15	470.87	380.18	8.9	2568.39
26		3.6	150.02	67.07	40.12	242.38	156.41	194.51	7.86	1363.06
27	Qipanjing	24.89	583	134.11	68.77	206.43	569.65	804.58	7.64	3773.97
28		40	633.66	145.95	56.83	223.83	680.79	813.42	7.7	4079.67
29		4.2	504	98.61	78.33	240.64	530.96	627.75	8.17	3300.16
30		6.15	580	138.06	44.89	252.82	719.48	583.54	8.45	3685.09
31		5.6	680	94.67	85.49	142.07	694.78	822.26	8.05	4041.53
32		84.06	630	82.83	75.94	131.05	629.75	751.53	7.93	3770.39
33		81.48	900.4	69.42	88.36	188.45	953.27	1069.82	7.76	5260.19
34		3.5	604	114.39	121.31	212.23	617.4	884.15	7.94	4044.69

Note: Unit of cation and anion concentration is mg/L, and pH is dimensionless.

The detection results and direction of groundwater runoff were employed to generate seven conventional ion (Ca^{2+}, Mg^{2+}, Na$^+$, K$^+$, Cl$^-$, SO$_4^{2-}$, HCO$_3^-$) concentration, pH, and TDS contour maps utilising Suffer software (Suffer 8.0) (Figure 3). The recharge directions of Ordovician limestone water can be classified into two categories. The initial category encompasses the flow from Zhuozishan Mountain to Gongdeer Mountain, subsequently extending in a south–north direction. The second category comprises the recharge from Zhuozishan Mountain to the south. It is evident that the distribution characteristics of the aforementioned ions (Na$^+$ + K$^+$, HCO$_3^-$, Cl$^-$, SO$_4^{2-}$, TDS, and pH) generally increase from the recharge area to the discharge area. In contrast, the distribution characteristics of Ca^{2+} and Mg^{2+} demonstrated an inverse relationship. This phenomenon is particularly evident in the central region. The contour distribution of the various indicators is relatively dense in the northern and southern parts, indicating significant variation in the hydrochemical indicators.
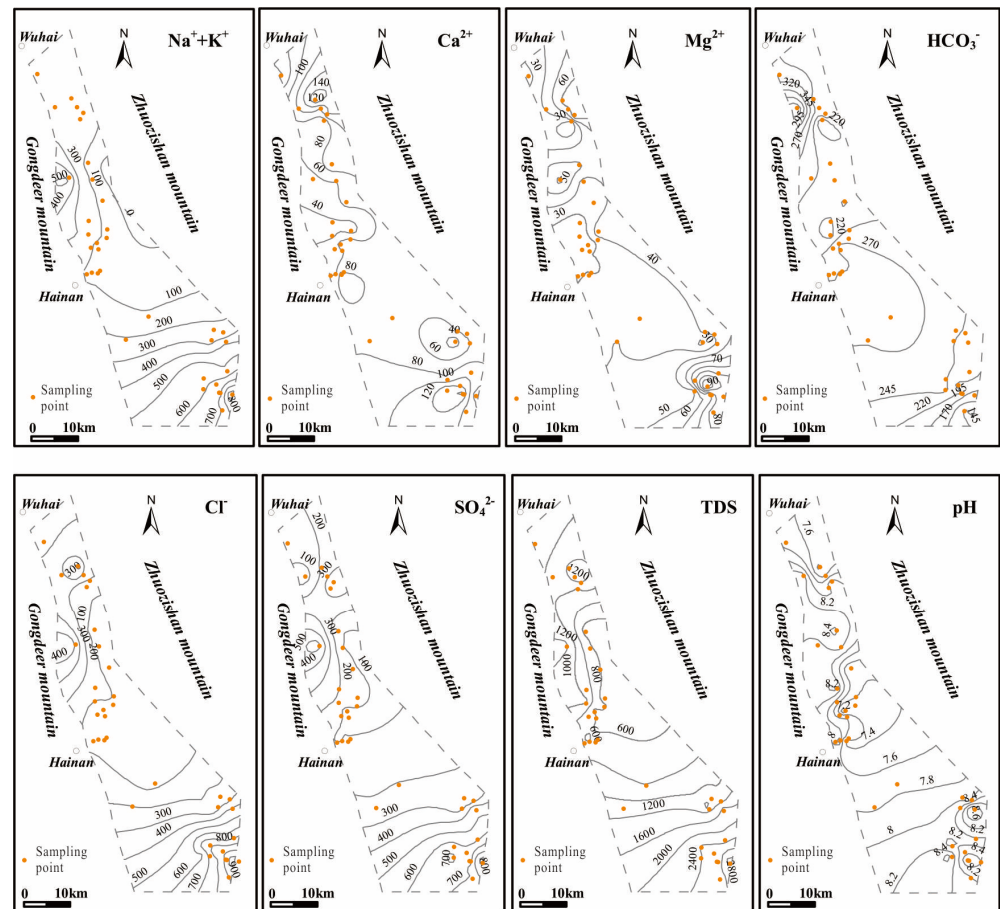
Figure 3. Contour of the concentration of ions.

3.2. Hydrochemical Types

The Piper trilinear diagram is an effective tool for identifying the relationships between diverse dissolved components and various types of groundwater, based on their hydrochemical characteristics [16,17]. As illustrated in the Piper diagram (Figure 4), the predominant hydrochemical types of Ordovician limestone water in the Zhuozishan coalfield were identified as $SO_4 \cdot Cl-Ca \cdot Na$, $HCO_3 \cdot SO_4 \cdot Cl-Ca \cdot Na$, $HCO_3 \cdot Cl-Ca \cdot Na$, and HCO_3^- $Ca \cdot Na$. The hydrochemical types of groundwater can be classified according to the direction of groundwater runoff, resulting in two distinct categories, as illustrated in the figure. The hydrochemical type undergoes a transformation from $SO_4 \cdot Cl-Ca \cdot Na$ in the upstream region to $HCO_3 \cdot SO_4 \cdot Cl-Ca \cdot Na$, $HCO_3 \cdot Cl-Ca \cdot Na$, or HCO_3-$Ca \cdot Na$ as the groundwater flows from the Zhuozishan Mountain to the Gongdeer Mountain and then in a north–south direction. Secondly, the runoff from the Zhuozishan Mountain to the south consistently exhibits the hydrochemical type $SO_4 \cdot Cl-Ca \cdot Na$. As illustrated in the TDS contour map, the TDS concentration of the runoff originating from the Zhuozishan Mountain and traversing the Gongdeer Mountain before continuing in a northerly direction ranges between 1200 and 1400 mg/L. In contrast, the concentration of the runoff directed southwards falls within the 600–1000 mg/L range. The concentration of total dissolved solids (TDSs) in the runoff from the Zhuozishan Mountain to the south is 1200–2800 mg/L, exhibiting a gradual increase. It is evident that the proportion of HCO_3^- (mg equivalent) increases, while the TDS concentration undergoes only slight fluctuations throughout the runoff process from the Zhuozishan Mountain to the Gongdeer Mountain and subsequently to the south or north. During the runoff process from the Zhuozishan Mountain to the south, the hydrochemical type remains unaltered, yet the TDS concentration rises gradually, suggesting that hydrochemical reactions occur within the groundwater during this process.
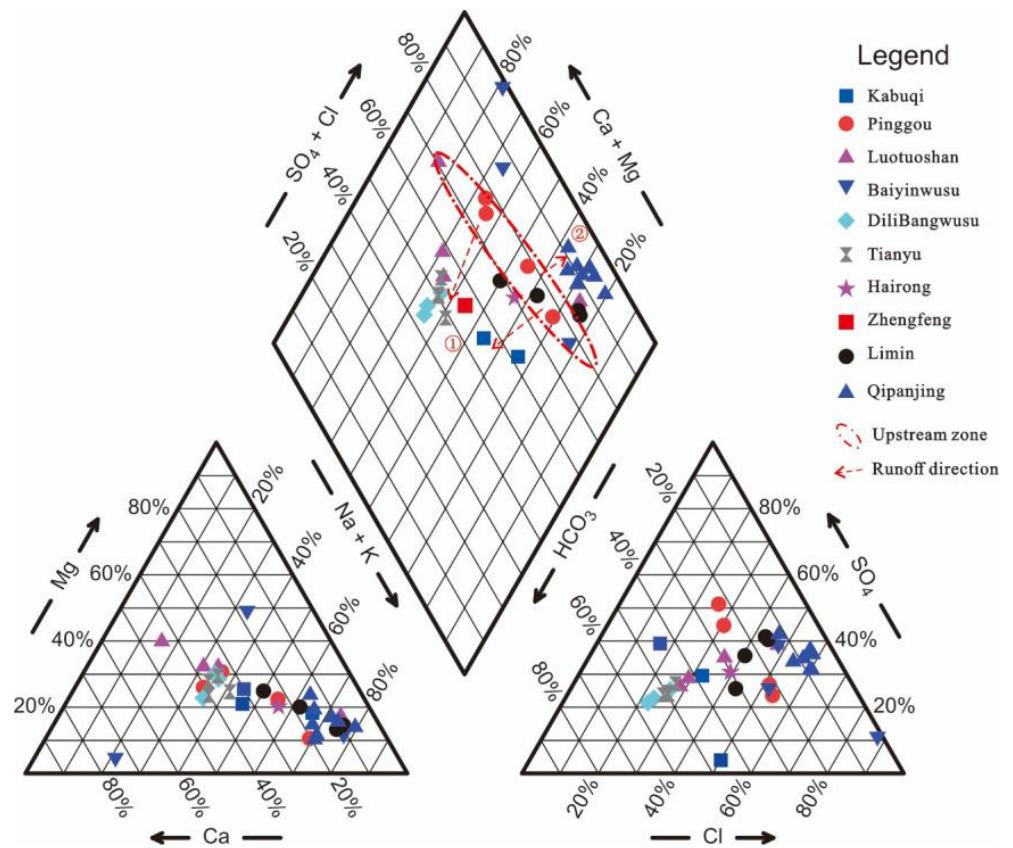
Figure 4. Piper trilinear diagram of Ordovician limestone water in Zhuozishan coalfield. (① The primary control action in this case is rock weathering; ② The control action of groundwater shifts from rock dominance to evaporation domi-nance).

4. Discussion

4.1. Rock Weathering Action

The Gibbs diagram [18] constituted an invaluable tool for the initial investigation of the processes involved in the formation of surface water, and it has since become a widely employed methodology in groundwater research [19]. The principal control factors can be classified into three categories: those pertaining to evaporation and concentration, those associated with rock weathering, and those related to precipitation (Figure 5). The analytical results demonstrate that the groundwater hydrochemical process can be divided into two categories. The first category comprises runoff from Zhuozishan Mountain, which flows north–south. The primary control action in this case is rock weathering. The second category encompasses runoff from Zhuozishan Mountain to the south. In this instance, the control action of groundwater shifts from rock dominance to evaporation dominance, progressing from the upstream to the downstream. However, the Ordovician limestone groundwater is located at a considerable depth, and thus will not be subjected to evaporation and concentration. It can thus be postulated that a reverse cation exchange effect may occur in the runoff direction from Zhuozishan Mountain to the south, resulting in an increase in the concentration of certain ions.
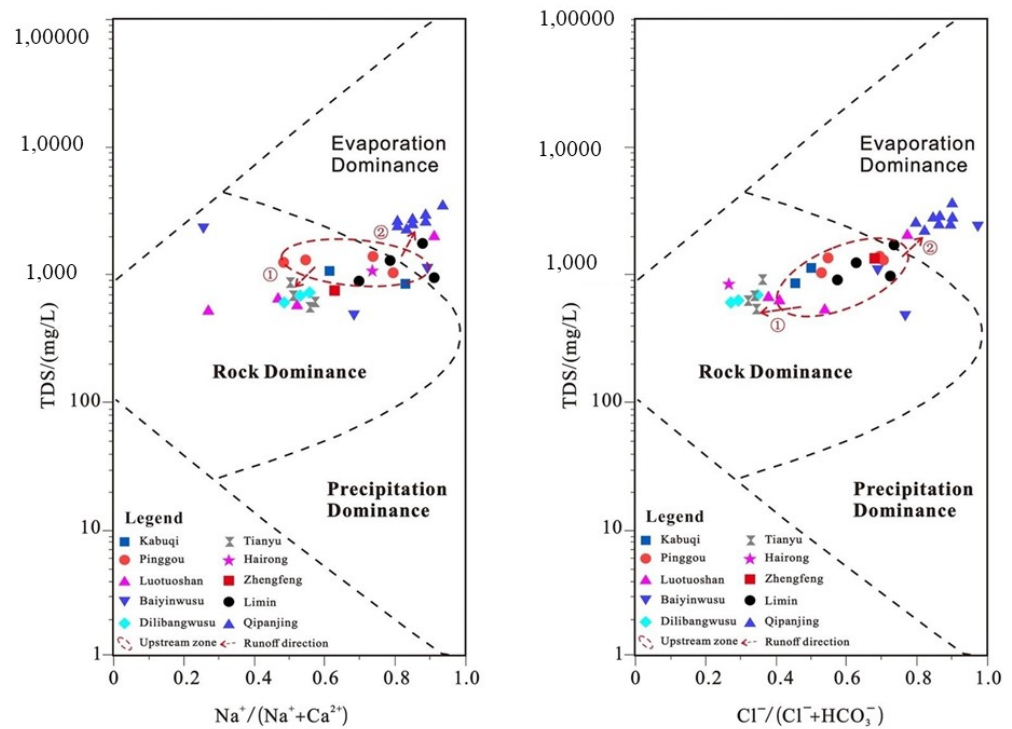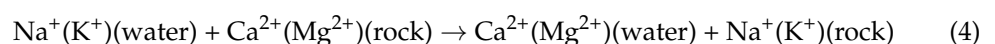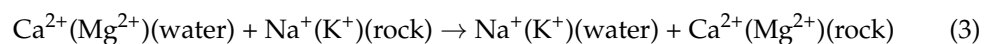
Figure 5. Gibbs diagram of Ordovician limestone water. (① The primary control action in this case is rock weathering; ② The control action of groundwater shifts from rock dominance to evaporation domi-nance).

Cation exchange is also a vital process affecting groundwater chemical features [20–22]. Typically, two chloro-alkaline indices (*CAI*-1 and *CAI*-2) proposed by Schoeller (1965) [23] are important ways of researching the occurrence of cation exchange, where the units of all ions are meq/L. When *CAI*-1 and *CAI*-2 are negative, this indicates that an ion exchange effect occurs, in which Na^+ and (or) K^+ in water-bearing media are replaced by Ca^{2+} and (or) Mg^{2+} in groundwater. But when *CAI*-1 and *CAI*-2 are positive, the reverse cation exchange effect occurs [24]. The calculation equations of *CAI*-1 and *CAI*-2 can be estimated as follows [25]:

$$CAI - 1 = \left(Cl^- - \left(Na^+ + K^+\right)\right)/Cl^- \tag{1}$$

$$CAI - 2 = \left(Cl^- - \left(Na^+ + K^+\right)\right)/\left(HCO_3^- + SO_4^{2-} + CO_3^{2-} + NO_3^-\right) \tag{2}$$

In this study, samples from the north and central parts of Zhuozishan coalfield groundwater are drawn in the lower left area, whereas samples from the south part are mostly in the upper right area of Figure 6a. This suggests that an ion exchange effect (Equation (3)) occurs in the runoff from the Zhuozishan to Gongdeer coalfield and then in a south–north direction, and reverse cation exchange (Equation (4)) occurs in the runoff from Zhuozishan coalfield to the south. In other words, groundwater cation exchanges of these two parts occur in reverse.
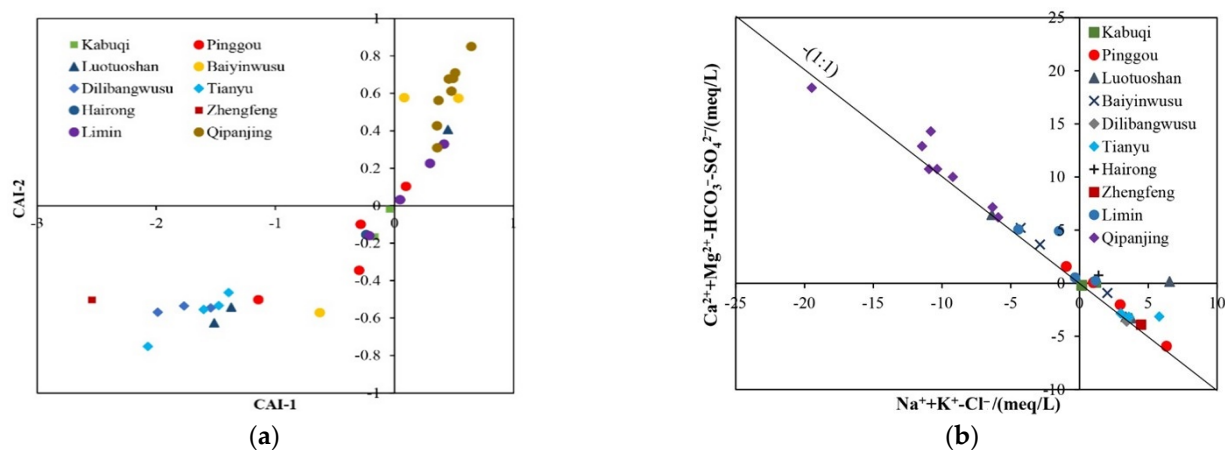
$$Ca^{2+}(Mg^{2+})(water) + Na^+(K^+)(rock) \rightarrow Na^+(K^+)(water) + Ca^{2+}(Mg^{2+})(rock) \tag{3}$$

$$Na^+(K^+)(water) + Ca^{2+}(Mg^{2+})(rock) \rightarrow Ca^{2+}(Mg^{2+})(water) + Na^+(K^+)(rock) \tag{4}$$

Figure 6. Chloro-alkaline indices of water (**a**) and $(Ca^{2+} + Mg^{2+} - HCO_3^- - SO_4^{2-})/(Na^+ + K^- - Cl^-)$ (**b**).

In order to verify the hypothesis of cation exchange reactions, the relationship between $(Na^+ + K^+ - Cl^-)$ and $[(Ca^{2+} + Mg^{2+}) - (HCO_3^- - SO_4^{2-})]$ was examined (Figure 6b). The values of $(Na^+ + K^+ - Cl^-)$ indicate the extent of Na^+ gains or losses resulting from halite dissolution [12]. Furthermore, the values of $[(Ca^{2+} + Mg^{2+}) - (HCO_3^- - SO_4^{2-})]$ demonstrate the extent of Ca^{2+} and Mg^{2+} gains or losses resulting from the dissolution of gypsum, calcite, and dolomite [26]. Figure 6a demonstrates that all groundwater samples are distributed along or in close proximity to the line with a slope of -1, indicating that the Ordovician limestone groundwater is subject to cation exchange. The samples from coal mines situated in the northern and central regions of the Zhuozishan coalfield are predominantly distributed in the fourth quadrant of the coordinate axis, whereas those from the southern area are primarily situated in the second quadrant of the coordinate axis. Furthermore, the distance from Zhuozishan Mountain (the source of groundwater recharge) is inversely proportional to the distance from the origin of the coordinates, indicating that the strength of the cation exchange effect increases with distance from the recharge area.

4.2. Main Ion Sources

The ratio of sodium to potassium and chloride can be employed as a means of investigating the sources of sodium and potassium in groundwater. The proximity of the samples to the 1:1 aquiline indicates that the primary sources of Na^+ and K^+ are halite dissolution [27]. Figure 7a demonstrates that groundwater samples from the south and north of the Zhuozishan coalfield exhibit a significant deviation from the 1:1 line, indicating that Na^+ and K^+ originate from halite dissolution and are minimally influenced by cation exchange.

Prior research has demonstrated that if sulphate rock dissolution represents the primary process within a groundwater system, the $(Ca^{2+} + Mg^{2+})/SO_4^{2-}$ ratio will be approximately equal to 1 [28,29]. Figure 7b demonstrates that the majority of the water samples are distributed above the 1:1 line at a ratio of approximately 2:1, indicating that the Ca^{2+} and Mg^{2+} in the Ordovician limestone groundwater are derived from carbonate or silicate dissolution, rather than sulphate minerals. Furthermore, if carbonate dissolution is the primary process in a groundwater system, the $(Ca^{2+} + Mg^{2+})/HCO_3^-$ ratio will be approximately 1. Figure 7c demonstrates that only a limited number of groundwater samples plot near the 1:1 line. The water samples from the southern and northern regions of the coalfield plot above the 1:1 line, whereas those from the central region are predominantly distributed below this line. In combination with Figure 7b,c, it can be concluded that the majority of Ca^{2+} and Mg^{2+} in the groundwater system is derived from silicate dissolution, with a smaller contribution from other rock types.
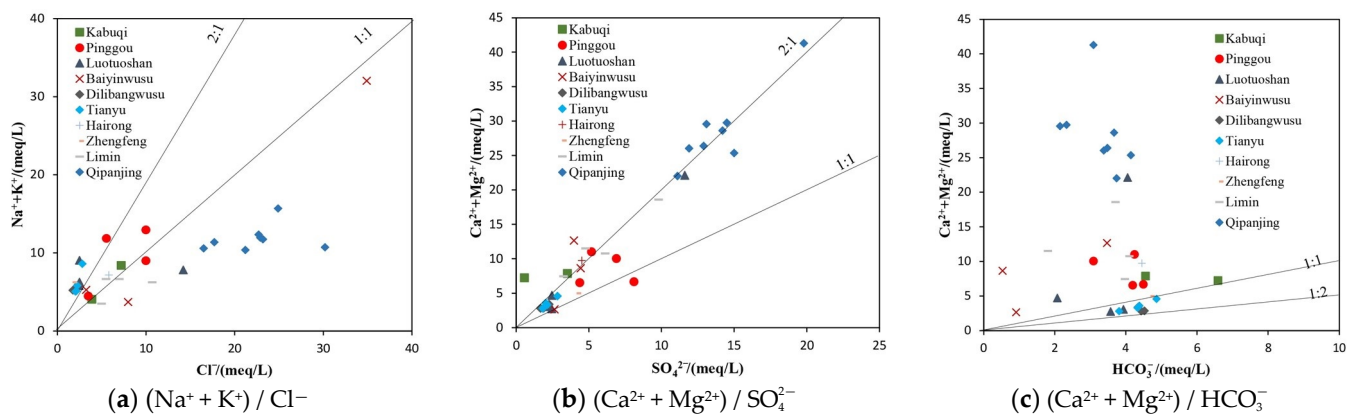
Figure 7. Ratio relation of main ions in Ordovician limestone water.

4.3. Mechanisms of Hydeogeochemistry

Based on the previous sections, the Ordovician groundwater runoff in the Zhuozishan coalfield can be classified into two primary flow directions. One direction flows from Zhuozishan Mountain to Gongdeer Mountain, then continues in a north–south direction. The other direction originates from Zhuozishan Mountain and flows southward. Furthermore, hydrochemical analysis reveals that the Zhuozishan coalfield can be divided into three distinct regions: the "northern", "central", and "southern" sectors. The hydrochemical processes active in each of these regions are summarised as follows:

4.3.1. Northern Part

Following replenishment from Zhuozishan Mountain, the groundwater in the northern region flows westward. The groundwater then traverses the Kabuqi syncline, reaching the eastern flank of Gongdeer Mountain, where it encounters a water-blocking fracture. As a result, the groundwater alters its course to a north–south direction within the syncline. The sudden change in the direction of groundwater runoff causes the formation of a retention area of groundwater in the Kabuqi syncline. Furthermore, the constant recharge of groundwater results in a disruption to the direction of groundwater runoff in the retention area (Figure 8). Consequently, groundwater flows to the downstream area for an extended period, resulting in a series of interconnected and non-uniform contours of hydrochemical indices (Figure 4). This consequently leads to a more complex hydrochemical typology and process in this region.

4.3.2. Central Part

The groundwater in the central region is derived from two primary sources: runoff from the north and the recharge area of Zhuozishan Mountain. The former flows downstream through the fault zone, while the latter contributes to the groundwater flow in the southern part of the Zhuozishan coalfield. It can therefore be concluded that the groundwater in the central region has not been obstructed by geological structures and that the direction of runoff remains unchanged. The regular alteration in the contours of the hydrochemical indices (Figure 4) is characterised by a hydrochemical type dominated by $HCO_3 \cdot Cl\text{-}Ca \cdot Na$ (Figure 5). The hydrochemical process is primarily controlled by rock weathering (Figure 6) and cation exchange (Figure 7).
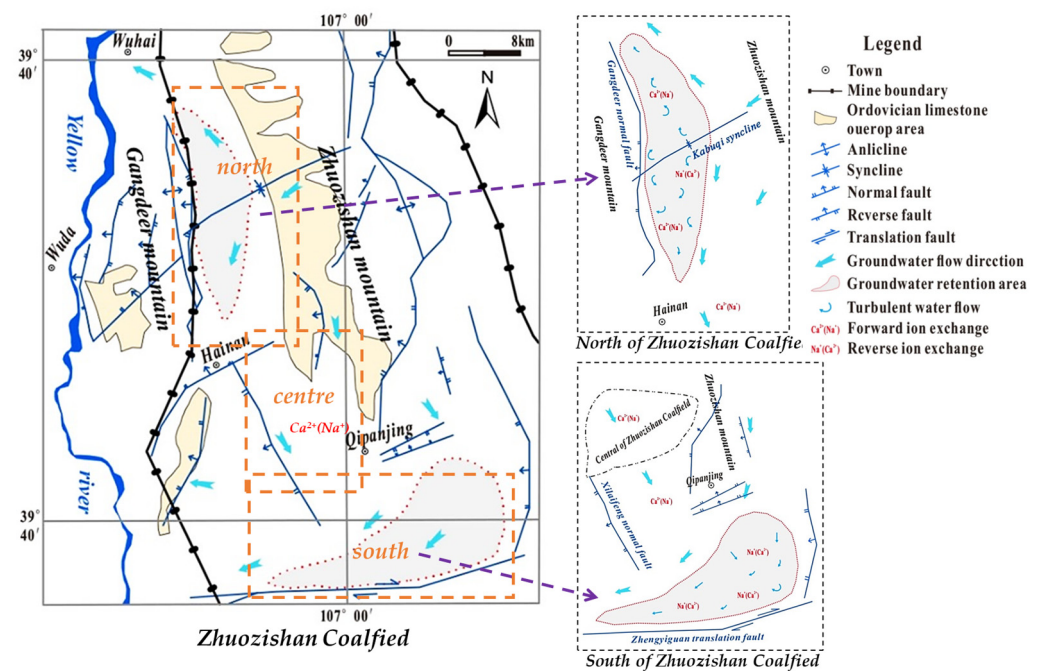
Figure 8. Schematic diagram for the formation of Ordovician groundwater in Zhuozishan coalfield.

4.3.3. Southern Part

The groundwater in the southern region is derived primarily from the runoff in the north or the recharge area of Zhuozishan Mountain. However, as a result of the gradual deepening of strata in the south and the blocking of the Zhengyiguan strike-slip fault, a retention zone has been formed (Figure 8). Subsequently, groundwater flows in a south-westerly direction. Consequently, the hydrochemical indices display a dense and regular distribution pattern, as illustrated in Figure 3. The hydrochemical type is consistently dominated by the $SO_4 \cdot Cl\text{-}Ca \cdot Na$ type (Figure 4), with a more prominent reverse cation exchange effect (Figure 7).

5. Conclusions

The characteristics of the Ordovician limestone groundwater in the Zhuozishan mining area, located in northwestern China, as well as its hydrochemical processes and mechanisms, were analysed through a series of groundwater samples collected from the Zhuozishan mining area. The conclusions of the study can be summarised as follows:

(1) The hydrogeochemical characteristics of the Ordovician limestone groundwater in Zhuozishan are closely related to the direction of groundwater runoff. The concentrations of Na^+, K^+, Cl^-, SO_4^{2-}, HCO_3^-, TDS, and pH increase from the recharge area to the discharge area, whereas those of Ca^{2+} and Mg^{2+} decrease. The concentration contours of Na^+, K^+, Cl^-, SO_4^{2-}, HCO_3^-, Ca^{2+}, Mg^{2+}, TDS, and pH are densely distributed in the north and south of Zhuozishan, indicating that these chemical indices show significant variations.

(2) A significant alteration in the hydrogeochemical types of the previous runoff direction (from Zhuozishan Mountain to Gongdeer Mountain and then to the south–north directional runoff) can be observed, whereas the latter is consistently dominated by $SO_4 \cdot Cl\text{-}Ca \cdot Na$. This indicates different hydrochemical effects have occurred in their runoff process. Furthermore, according to the analysis of the Gibbs diagram and chloro-alkaline index, it can be concluded that the formation processes of groundwater in the two runoff directions are governed by distinct mechanisms. Specifically, the former is affected by rock weathering action and cation exchange, whereas the latter is controlled by rock weathering action to the evaporation concentration and reverse cation exchange. In terms of ion sources, Ca^{2+} and Mg^{2+} mainly originate from the silicate dissolution, while Na^+ and K^+ are mainly derived from cation exchange, with little halite dissolution.

(3) The formation of three hydrochemical characteristic areas with different flow directions has been identified in the study area. In the northern part, the groundwater is influenced by a complex geological structure, resulting in a retention area and disordered runoff direction, with intricate hydrochemical types and processes. The central zone, however, is unaffected by geological constraints and has a uniform flow direction, resulting in a simpler hydrochemical type, mainly influenced by rock weathering and cation exchange. In the southern part, deepening of the strata and fault blockage result in a hydrochemical type similar to that of the recharge area and strong reverse cation exchange.

Author Contributions: Conceptualisation, S.W. and T.W.; methodology, T.W.; software, Z.Y. and H.T.; validation, S.W. and T.W.; formal analysis, S.W., T.W. and H.L.; investigation, F.X. and K.Z.; data curation, K.Z., Z.L. and F.X.; writing—original draft preparation, S.W. and T.W.; writing—review and editing, S.W.; visualisation, H.L., H.T. and Z.Y.; supervision, S.W. and T.W. All authors have read and agreed to the published version of the manuscript.

Data Availability Statement: The data used to support the findings of this study are available from the corresponding author upon request.

Conflicts of Interest: Author Shidong Wang, Tiantian Wang, Zhibin Yang, Hongwei Tang, Hanjiang Lv, Feng Xu, Kaipeng Zhu, and Ziyuan Liu were employed by the company Technology & Engineering, Xi'an Research Institute of China Coal (Group), Corp. The remaining authors declare that the research was conducted in the absence of any commercial or financial relationships that could be construed as a potential conflict of interest.

References

1. Rajesh, R.; Brindha, K.; Elango, L. Groundwater quality and its hydrochemical characteristics in a shallow weathered rock aquifer of southern India. *Water Qual. Expo. Health* **2015**, *7*, 515–524. [CrossRef]
2. Wang, T.T.; Yang, J.; Li, G.Q. The hydrogeochemical characteristics and formation mechanism of high-fluoride mine water. *J. Clean. Prod.* **2023**, *430*, 139671. [CrossRef]
3. Jin, D.; Wang, T.; Zhao, B.; Li, D.; Zhou, Z.; Shang, H. Distribution characteristics and formation mechanism of high salinity groundwater in northeast Ningdong Coalfield. *Coal Geol. Explor.* **2022**, *50*, 118–127. [CrossRef]
4. Wang, T.; Jin, D.; Yang, J. Heavy metal pollution characteristics and source analysis of water drainage from a mine in Inner Mongolia. *Coal Geol. Explor.* **2021**, *49*, 45–51. [CrossRef]
5. Wang, H.; Dong, S.; Shang, H.; Wang, T.; Yang, J.; Zhao, C.; Zhnag, Q.; Zhou, Z.; Liu, J.; Hou, Y. Domestic and foreign progress of mine water treatment and resource utilization. *Coal Geol. Explor.* **2023**, *51*, 222–236. [CrossRef]
6. Wang, T.; Zhao, W.; Wang, Z.; Zhou, Z.; Yang, J.; Xu, F.; Xue, J.; Li, G. Occurrence, Main Source and Health Risks of Fluorine in Mine Water. *Expo. Health* **2024**, 1–14. [CrossRef]
7. Jin, D.; Li, C.; Liu, Y.; Cao, H.; Ren, D.; Wang, H.; Zhang, J.; Huang, Y.; Yang, G.; Guo, K.; et al. Characteristics of roof water hazard of coal seam in Huanglong Coalfield and key technologies for prevention and control. *Coal Geol. Explor.* **2023**, *51*, 205–213. [CrossRef]
8. Wang, T.; Jin, D.; Xue, J.; Ji, H.; Shang, H.; Zhou, Z.; Yang, J.; Cao, Y. Source and release law of fluorine in water-rock system of coal mine goaf in contiguous area of Shaanxi and Inner Mongolia. *Coal Geol. Explor.* **2023**, *51*, 252–262. [CrossRef]
9. Gu, H.; Lai, X.; Tao, M.; Momeni, A.; Zhang, Q. Dynamic mechanical mechanism and optimization approach of roadway surrounding coal water infusion for dynamic disaster prevention. *Measurement* **2023**, *223*, 113639. [CrossRef]
10. Zhang, C.; Luo, B.; Xu, Z.; Sun, Y.; Feng, L. Research on the Capacity of Underground Reservoirs in Coal Mines to Protect the Groundwater Resources: A Case of Zhangshuanglou Coal Mine in Xuzhou, China. *Water* **2023**, *15*, 1468. [CrossRef]
11. Sun, W.; Zhou, W.; Jiao, J. Hydrogeological Classification and Water Inrush Accidents in China's Coal Mines. *Mine Water Environ.* **2016**, *35*, 214–220. [CrossRef]
12. Wang, Y.; Shi, L.; Wang, M.; Liu, T. Hydrochemical analysis and discrimination of mine water source of the Jiaojia gold mine area, China. *Environ. Earth Sci.* **2020**, *79*, 123. [CrossRef]
13. Li, P.; Tian, R.; Liu, R. Solute geochemistry and multivariate analysis of water quality in the Guohua phos-phorite mine, Guizhou Province, China. *Expo. Health* **2018**, *11*, 81–94. [CrossRef]
14. Yang, Z.B. Prevention and Countermeasures of Floor Water Disaster in Lower-group Coalseam Mining in Zhuozishan Coalfield. *Coal Min. Technol.* **2015**, *20*, 133–136. (In Chinese) [CrossRef]

15. Wang, S.D.; Zhu, K.P.; Tang, H.W. Evolution Mechanism and Circulation Characteristics of Ordovician Lime-stone Water in Zhuozishan Coalfield. *Min. Saf. Environ. Prot.* **2017**, *44*, 116–120. [CrossRef]

16. Ministry of Environmental Protection of the PR China. *Water Quality Sampling—Technical Regulation of the Preservation and Handling of Samples*; HJ 493–2009; China Environmental Science Press: Beijing, China, 2009. (In Chinese)

17. Tiwari, A.K.; Singh, A.K.; Singh, M.P. Hydrogeochemical analysis and evaluation of surface water qual-ity of pratapgarh district, uttar pradesh, India. *Appl. Water Sci.* **2017**, *7*, 1609–1623. [CrossRef]

18. Shakya, B.M.; Nakamura, T.; Shrestha, S.D.; Nishida, K. Identifying the deep groundwater recharge processes in an intermountain basin using the hydrogeochemical and water isotope characteristics. *Hydrol. Res.* **2019**, *50*, 1216–1229. [CrossRef]

19. Gibbs, R.J. Mechanisms controlling world water chemistry. *Science* **1970**, *170*, 795–840. [CrossRef]

20. Li, P.; Li, X.; Meng, X.; Li, M.; Zhang, Y. Appraising groundwater quality and health risks from contamination in a semiarid region of northwest China. *Expo. Health* **2016**, *8*, 361–379. [CrossRef]

21. Pehlivan, R. Potability and Hydrogeochemical Characteristics of the Karasu Stream Water, Sakarya, Turkey. *Geochem. Int.* **2020**, *58*, 1075–1081. [CrossRef]

22. Zhang, B.; Zhao, D.; Zhou, P.; Qu, S.; Liao, F.; Wang, G.C. Hydrochemical Characteristics of Groundwater and Dominant Water–Rock Interactions in the Delingha Area, Qaidam Basin, Northwest China. *Water* **2020**, *12*, 836. [CrossRef]

23. Shi, Z.; Liao, F.; Wang, G.; Xu, Q.; Mu, W.; Sun, X. Hydrogeochemical Characteristics and Evolution of Hot Springs in Eastern Tibetan Plateau Geothermal Belt, Western China: Insight from Multivariate Statistical Analysis. *Geofluids* **2017**, *2017*, 6546014. [CrossRef]

24. Schoeller, H. Qualitative Evaluation of Groundwater Resources. In *Methods and Techniques of Groundwater Investigations and Development*; UNESCO: Paris, France, 1965; pp. 54–83.

25. Liu, J.; Gao, Z.; Wang, Z.; Xu, X.; Su, Q.; Wang, S.; Qu, W.; Xing, T. Hydrogeochemical processes and suitability assessment of groundwater in the Jiaodong Peninsula, China. *Environ. Monit. Assess.* **2020**, *192*, 1–17. [CrossRef]

26. Hou, G.C.; Lin, X.Y.; Su, X.S.; Wang, X.Y.; Liu, J. Groundwater System in Ordos Cretaceous Artisan Basin. *J. Jilin Univ. (Earth Sci. Ed.)* **2006**, *36*, 391–398. (In Chinese) [CrossRef]

27. Ke, X.M.; Li, Y.J.; Wang, W. Hydrogeochemical characteristics and processes of thermokarst lake and groundwater during the melting of the active layer in a permafrost region of the Qinghai-Tibet Plateau, China. *Sci. Total Environ.* **2022**, *851*, 158183. [CrossRef]

28. Li, P.; Wu, J.; Qian, H.; Zhang, Y.; Yang, N.; Jing, L.; Yu, P. Hydrogeochemical characterization of groundwater in and around a wastewater irrigated forest in the southeastern edge of the Tengger Desert, northwest China. *Expo. Health* **2016**, *8*, 331–348. [CrossRef]

29. Li, P.; Wu, J.; Rui, T.; Song, H.; He, X.; Xue, C.; Kang, Z. Geochemistry, Hydraulic Connectivity and Quality Appraisal of Multilayered Groundwater in the Hongdunzi Coal Mine, Northwest China. *Mine Water Environ.* **2018**, *37*, 1–16. [CrossRef]